Article

pubs.acs.org/Biomac

# Sequence-Defined Peptidocopolymers: The Effect of Small Molecular Linkers

Yijiang Liu,[†] Yu Kang,[‡] Jue Wang,[†] Zheyu Wang,[†] Guosong Chen,*[,†] and Ming Jiang[†]

[†]The State Key Laboratory of Molecular Engineering of Polymers and Department of Macromolecular Science, Fudan University, Shanghai, 200433 China

[‡]College of Pharmaceutical Sciences, Zhejiang University, Hangzhou, Zhejiang 310058, People's Republic of China

Supporting Information

**ABSTRACT:** In this paper, the contribution of nonpeptido small molecular linkers to the properties of sequence-defined peptidocopolymers was investigated. We synthesized four novel bioinspired peptidocopolymers (**P1**−**P4**) based on elastin motif pentapeptide (Gly-Pro-Gly-Gly-Ala) by step growth polymerization. Small molecular linkers, including tetraethylene glycol (**M1**), adipic acid (**M2**), isophthalic acid (**M3**), and terephthalic acid (**M4**) with different length and flexibility are employed to tune the conformation, physical, and mechanical properties of the corresponding peptidocopolymers **P1**−**P4** respectively. Raman spectroscopy, solid state NMR, and circular dichroism spectroscopy were used to characterize the conformation of the four peptidocopolymers. The experimental results were further confirmed by molecular dynamics simulation of typical **P2** and **P4** with different repeating units. High ratio of $\beta$-turn conformation was observed in **P2** due to flexible linker **M2**; while affected by the hydrophobic and rigid **M4** linker, **P4** retained less $\beta$-turn conformation and showed drastic difference on macroscopic properties. These simple step growth synthesis techniques provide an efficient approach toward a broad range of bioinspired peptidocopolymers, which takes a further insight into the significant effect of nonpeptido linkages toward chemical-synthesized peptidocopolymers.

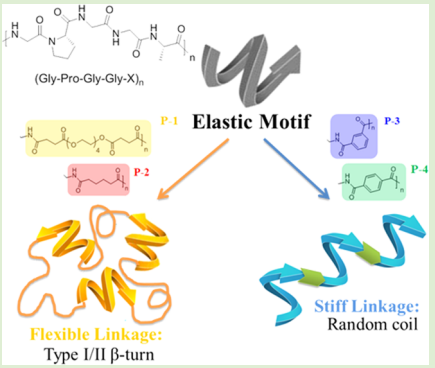


## INTRODUCTION

Biomaterials based on peptides are promising for biomedical applications,[1,2] including tissue engineering scaffold,[3,4] drug carriers[5] and gene delivery agents,[6,7] due to their great biocompatibility, degradability[8] and functionality.[9] There are mainly two types of peptide-based materials, polypeptides and sequence-controlled peptides. The former are synthetic polymers made by polymerization of amino acid monomer, while the latter are synthesized via recombinant DNA technique[10] or solid phase peptide synthesis.[11] Both of these techniques have achieved great success. By using living polymerization, polypeptides can be easily made to a large molar mass in a large scale, which is a solid basis for their further applications in biomaterials.[12] However, the type of amino acids in the resultant polypeptide is limited, which is far from the natural state of proteins. To synthesize sequence-controlled peptide materials that are more similar to their natural analogues, step-by-step biological or chemical methods have been employed. Unfortunately, both of them still suffer from labor-consuming and low yielding problems.

In order to synthesize sequence-defined peptidomaterials in a relatively high scale, Guan et al. proposed an elegant way to combine traditional polymer synthesis and step-by-step peptide synthesis techniques. By using step-growth polymerization via click chemistry, sequence-defined oligopeptide monomers were successfully polymerized, generating a new type of copolymers of polypeptide.[13−16] The resulted peptide copolymers showed similarity to native proteins not only in their conformation, but also in macroscopic properties. Similar approaches had also been used in preparing elastin-mimic hybrid polymers, which also showed promising potential as candidate scaffolds for tissue engineering.[3] However, by such polymer synthetic approach, the existence of nonpeptido species in the final products can hardly be avoided. Because a slight change of an amino acid on a certain position may largely influence protein conformation and usually results in different properties and functionality, the presence of the nonpeptido units in the copolymers may cause even larger effects.[17−19] Although their conformation similar to native protein was reported in most of pervious reported peptide copolymers, the effect of the nonpeptido species such as small molecular linker and five-membered triazole ring were seldom mentioned.[10]

The conformation of peptides or proteins may be affected by their chemical environment.[20] Among them, dynamic $\beta$-turn structure formed by intramolecular hydrogen bond is a vulnerable one. $\beta$-turns are one of the most common types of nonrepetitive structure in proteins, which provide a direction change of the peptide chain and key sites of molecular

Received: October 7, 2015
Revised: November 2, 2015





DOI: 10.1021/acs.biomac.5b01348
Biomacromolecules XXXX, XXX, XXX−XXX

**Scheme 1. Synthesis Steps of the Four Peptidocopolymers P1−P4 (DIPEA: *N,N*-Diisopropyl Ethylamine)**

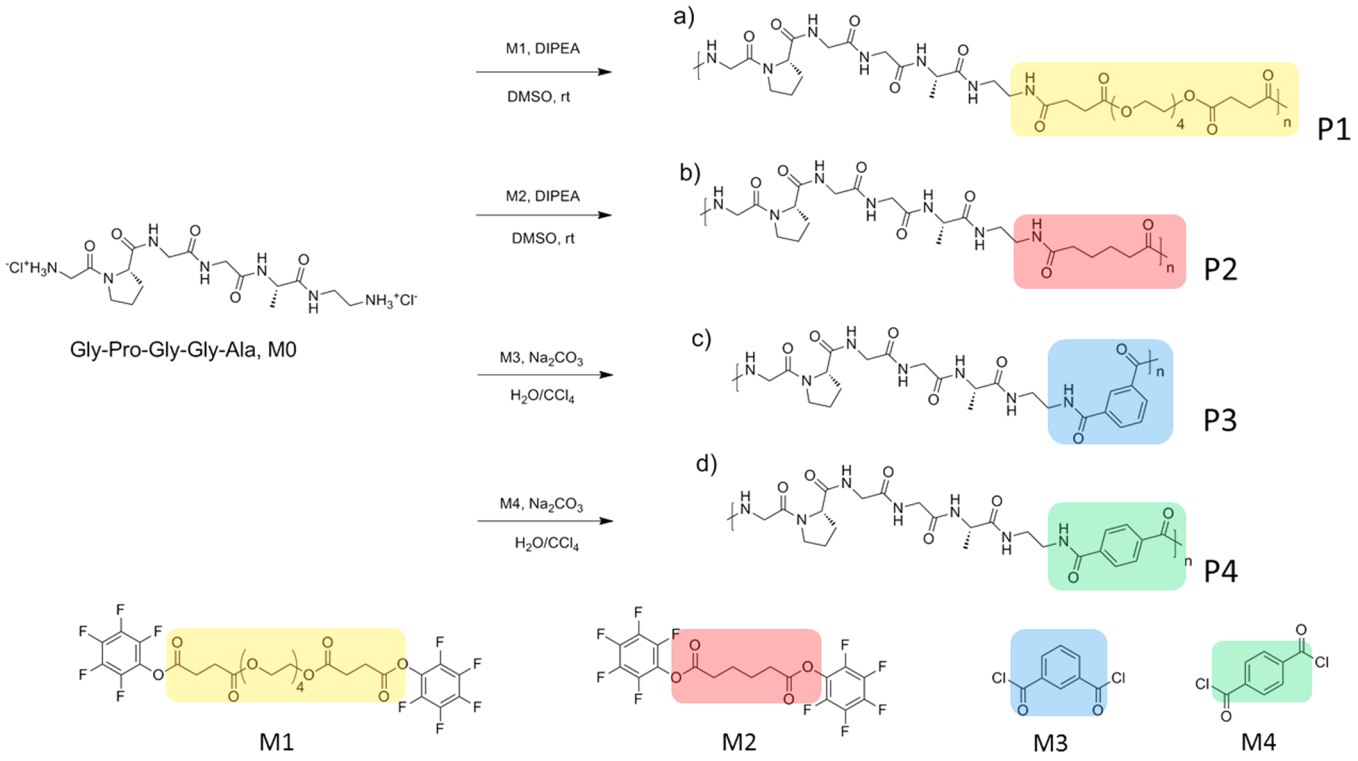


recognition.[21] Among different types of $\beta$-turn found in proteins, type I and II are commonly found in nature (Supporting Information Figure S1), of which typical internal hydrogen bonds were formed by $H_{(1)}...O_{(5)}$ and $H_{(4)}...O_{(2)}$ of the standard pentapeptide repeating unit.[24] Among many $\beta$-turn rich proteins, the elastins, which conferring elasticity to tissues and organs, have mostly been studied in recent years.[22] More specifically, they are featured by repeating unit VPGVG (Val-Pro-Gly-Val-Gly) and GPGGA (Gly-Pro-Gly-Gly-Ala) in mammal or silk fibers[23,24] (Supporting Information Figure S2). As reported by previous works, these repeating units are expected to adopt $\beta$-turn conformation in most conditions regardless of their chemical environment.[10,25−27] However, considering the vulnerable nature of $\beta$-turns, one may wonder that after polymerization whether such pentapeptide still adopts the previous local conformation in solution and bulk state or is affected by different nonpeptido small molecular linkers.

Herein, to study the conformation of $\beta$-turn pentapeptide after step-growth polymerization, sequence-defined copolymers based on the elastin motif GPGGA and different small molecular linkers were synthesized and studied with emphasis on the effect of the nonpeptide component on peptide conformation. Four typical small molecular linkers, that is, tetraethylene glycol (TEG), adipic acid, isophthalic acid and terephthalic acid with different length, flexibility, and conformation, are employed to link the pentapeptide GPGGA. All of the four small molecular linkers are wildly used in polymer material synthesis, among which TEG and adipic acid were chosen as polar and flexible linkers between peptide units with different length. In contrast, isophthalic and terephthalic acid were more rigid, hydrophobic with strong $\pi-\pi$ interaction. The resulting hybrid copolymers were named *peptidocopolymer*, which is featured by the well-defined peptide sequence in the presence of the chemical linkers. An advantage of the peptidocopolymer is the employment of metal-free step-growth[28−30] copolymerization to avoid copper ions, which were believed to have some unavoidable effect on conformation of synthetic peptides.[10] Taking advantage of Raman spectroscopy and solid state NMR, conformation of four peptidocopolymers was characterized, and the results were further confirmed by molecular dynamics (MD) simulation. The macroscopic properties of the peptidocopolymers were also studied by stress−strain analysis to demonstrate different contributions of the nonpeptido linkers to mechanical performance of the final material.

## EXPERIMENTAL METHODS

**Materials.** All chemicals including 1-(3-(dimethylamino)propyl)-3-ethylcarbodiimide hydrochloride (EDC), 1-hydroxybenzotriazole (HOBT), ethyldiisopropylamine (DIPEA), pentafluorophenol (PFp), and all modified amino acids were purchased from J&K Chemical, TCI and GL Biochem (Shanghai) and used without further purification. Anhydrous solvent were distilled after stirring with calcium hydride for more than 4 h.

**Characterization Methods.** $^1$H and $^{13}$C NMR spectra were taken on 400 MHz Bruker AVANCE III HD, and the acquired NMR data were analyzed with MestRe Nova software. Chemical shift values were referenced using the solvent peak at DMSO-$d_6$ (2.50) or $CDCl_3$ (7.27). Gel permeation chromatography (GPC) was carried out on a system comprising a Waters 1515 HPLC pump, TOSOH TSK gel $\alpha$-3000 and $\alpha$-2500 columns in series at 80 °C, Waters 2414 refractive index detector and Wyatt DAWN HELEOS II 18-angle laser light scattering detector. The eluent was DMF with 0.2% LiBr and flow rate was 1.0 mL/min. DSC measurements were performed on TA Q2000 differential scanning calorimeter at −20−160 °C in nitrogen atmosphere with the heating rate of 10 °C/min. Raman spectra were recorded using HORIBA JobinYvon XploRA spectrometer. The Spectra Physics model 164 argon ion laser was operated at 758 nm. Scattered light at right angle was analyzed on single spectrograph configuration with 1800 grooves/mm holographic grating and a holographic notch filter. The analysis of amide I band regions of


DOI: 10.1021/acs.biomac.5b01348
*Biomacromolecules* XXXX, XXX, XXX−XXX

Table 1. Physical Properties of Peptidocopolymers P1−P4

| copolymer | $M_n$ (kDa) | $M_w$ (kDa)[a] | DP | $M_w/M_n$ | conversion % | $T_g$ (°C, DSC)[b] |
|---|---|---|---|---|---|---|
| **M0** | | 0.47 | | | | 112 |
| **P1** | 11.0 | 15.9 | 21 | 1.44 | 95 | 42 |
| **P2** | 6.7 | 11.8 | 22 | 1.76 | 96 | |
| **P3** | 8.6 | 9.7 | 18 | 1.13 | 94 | |
| **P4** | 7.7 | 9.7 | 18 | 1.25 | 94 | |

[a]Absolute molar mass was measured by GPC-MALS, the corresponding d*n*/d*c* was measured by refractive index detector (RI). [b]DSC were performed under nitrogen atmosphere (temperature increasing speed: 10 °C per min).

Raman spectra was performed by curve fitting using mixtures of Gaussian and Lorentzian functions by PeakFit v4.12 software, and second derivative was used as a complementary approach to determine the location of the components. $^{13}C$ CPMAS NMR were carried out on prepared membranes using Bruker 400WB AVANCE III operated at 400 MHz with cross-polarization contact time of 4 ns, pulse repeat time of 2 s, accumulation of 800 scans, and high-power $^{1}H$-decoupling of 62.5 kHz during signal acquisition with a $^{1}H$ 90° pulse width of 4.0 us. Sample was spun at a rate of 10 kHz in a 4 mm spin rotor. The NMR peak was deconvoluted using mixtures of Lorentzian and Gaussian functions by PeakFit v4.12 software. Circular dichroism was performed on Chirascan-SF.3 CD-Stopped flow under 25 °C. Mechanical test was taken on CMT4104 Mechanical Test I instrument.

**General Procedure of the Amino Acid Coupling.** Typically, a solution of Boc-Gly-OH (6.00 g, 34.3 mmol), EDC (7.90 g, 41.2 mmol), HOBT (5.56 g, 41.2 mmol) in 150 mL of anhydrous dichloromethane (DCM) was cooled to −10 °C in ice-salt bath. To this solution, DIPEA (21.2 mL, 123.6 mmol) was slowly added, and then H-Pro-OMe (5.68 g, 34.3 mmol) was added. The solution was allowed to warm to room temperature and stirred overnight. Then the solution was washed with 30 mL of 2 M HCl and 30 mL of brine. The organic layer was dried over $MgSO_4$, and removed the solvent under reduced pressure. The crude product was purified by silica gel chromatography (2:1 ethyl acetate/hexane) to give 8.8 g (90%) Boc-Gly-Pro-OMe.

**General Procedure for Cleavage of the Methyl Group.** Typically, Boc-Gly-Pro-OMe (8.8 g, 32.8 mmol) was dissolved in 50 mL of methanol, and then 30 mL of $H_2O$ was added and cooled to 0 °C. To this solution, $LiOH{\cdot}H_2O$ (6.17 g, 154.3 mmol) was added. The mixture was allowed to warm to room temperature and stirred for 4 h. The solution was neutralized by adding 2 M $KHSO_4$ until pH 4−5. The methanol was removed under reduced pressure, and the aqueous solution was extracted with DCM (50 mL × 3). The organic layers were combined and dried over $MgSO_4$. The solvent was removed under reduced pressure to give 7.95 g (95%) of Boc-Gly-Pro-OH without further purification.

**General Procedure for Deprotection of the Boc Group.** Typically, Boc-Gly-Ala-OMe (8.2 g, 31.6 mmol) was cooled to 0 °C and 50 mL of 4 M HCl solution in ethyl acetate was added. The mixture was kept at 0 °C for a further 20 min while a large amount of white precipitates formed. The precipitate was filtered and washed with ethyl acetate several times to give 5.93 g (96%) of H-Gly-Ala-OMe.

**General Procedures for PFp Activated Ester Synthesis.** Typically, adipic acid (1.46 g, 10 mmol) and EDC (4.6 g, 24 mmol) was dissolved in 50 mL of DCM. The solution was allowed cool to 0 °C in an ice bath after which pentafluorophenol (PFp, 4.0 g, 22 mmol) that dissolved in 5 mL of DCM was added. The solution was allowed to warm to room temperature and was stirred for 5 h. After removal of the solvent under reduced pressure, the crude product was purified by silica gel chromatography (1:2 ethyl acetate/hexane) to give 4.5 g of **M2** (94%) (Scheme 1).

**General Procedure for Polymerization.** Typically, to a 10 mL vial was added the GPGGA pentapeptide monomer **M0** (0.472 g, 1 mmol, Scheme 1), DIPEA (1.0 mL, 6 mmol), and 2 mL of anhydrous DMSO. The mixture was allowed to stir at room temperature for 10 min after which **M1** (0.726 g, 1 mmol, Scheme 1) was added. The mixture was stirred at room temperature for 2 h, and 2 mL of methanol was added to dilute the viscous solution. The polymer was precipitated in ethyl ether, filtered, and dried under vacuum at 40 °C for 48 h to remove solvents to give 0.56 g **P1** (86%).

**Molecular Dynamics Simulation.** For MD simulation, the pentapeptide monomer **M0** (Scheme 1) was first set as the repeating unit, and a series of peptidocopolymers composed of up to four repeating units ($n$ = 1,2,4) were modeled independently in order to systematically investigate the conformational preferences of these copolymers integrated with different linkers **M2** and **M4**. For clarity, abbreviations **P2** and **P4** are continuously used in this part for the corresponding copolymers. The AMBER 03 force field[31] was used for the major part of this study, followed by a number of comparative simulations with the CHARMM 36 force field.[32] MD simulations were conducted with two simulation packages, Gromacs v. 4.5.5[33,34] and Amber 11,[35] that complied with the same explicit water model TIP3P.[36] MD simulations with implicit solvent were also conducted for comparison. More simulation details are shown in Supporting Information.

## RESULTS AND DISCUSSION

**Design, Synthesis, and Characterization of Peptidocopolymers.** To polymerize GPGGA pentapeptide, the end alanine was first extended with ethylenediamine to have amine at both of the pentapeptide ends (Scheme 1). For convenience, its hydrochloride salt was generated and used as the peptidomonomer (**M0**) in the step-growth copolymerization. To integrate flexible linkers (TEG and adipic acid) the reaction between pentafluorophenol (PFp) active ester and primary amine was used for copolymerization because of its high efficiency under mild condition. Thus, PFp-$PEG_4$-PFp (**M1**) and PFp-Adipic-PFp (**M2**) were used as the nonpeptido part to generate copolymer **P1** and **P2**, respectively. Because of the poor solubility of terephthalic and isophthalic PFp active esters in the most common solvent, interfacial copolymerization between their corresponding acyl chloride (terephthaloyl chloride, **M3**; Isophthaloyl chloride, **M4**) and amino end-group of pentapeptide were used to obtain **P3** and **P4**. Molar mass of the resulting polymers (**P1** to **P4**) was measured by gel permeation chromatography with multiangle light scattering detector (GPC-MALS) in DMF. **P1**, **P2**, **P3**, and **P4** gave absolute molar mass ($M_w$) as 15.9, 11.8, 9.7, and 9.7 kDa (Table 1, the d*n*/d*c* showed in Supporting Information Figure S3). The corresponding degree of polymerization (DP) of the four copolymers was listed in Table 1. Figure 1 and Supporting Information Figures S4−7 showed GPC traces of the four peptidocopolymers. **P1** and **P2** showed high solubility in water and other polar solvents due to their noncrystalline and hydrophilic nature. After integration with the hydrophobic and stiff aromatic rings in **P3** and **P4**, poor water solubility of the two polymers was observed, although they still can be dissolved in solvents with high polarity, such as DMF and DMSO. All copolymers began to decompose around 220 °C without melting as shown in their differential scanning calorimetry


DOI: 10.1021/acs.biomac.5b01348
Biomacromolecules XXXX, XXX, XXX−XXX

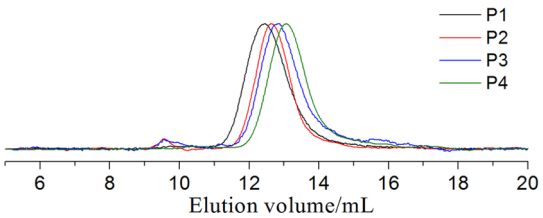


**Figure 1.** GPC traces of the four peptidocopolymers **P1**-**P4** monitored by MALS detector.

(DSC) curves (Supporting Information Figures S8−12). The glass transition ($T_g$) of **M0** appeared around 120 °C, while lower $T_g$ of **P1** and **P2** at 54 and 78 °C was detected, which may be attributed to the flexible linkers of TEG (**M1**) and adipci chain (**M2**). No obvious $T_g$ was found in **P3** and **P4**, mainly due to the stiffness induced by terephthalic (**M3**) and isophthalic (**M4**) linkers.

**Raman Spectroscopy of Peptidocopolymer in Bulk.** The conformation-sensitive amide I bands (1600−1700 $cm^{-1}$) in Raman spectroscopy have been widely used in studying the secondary structure of proteins.[37] The amide I bands of the four peptides **P1** to **P4** and monomer **M0** were observed around 1650−1670 $cm^{-1}$ (Supporting Information Figure S13). The board and asymmetric peaks indicated that the amide I bands were composed of several components representing different secondary structures. Thus, spectral decomposition was performed for further study. Typically for **M0**, three major components located near 1649, 1669, and 1691 $cm^{-1}$ were generated by the procedure described in Supporting

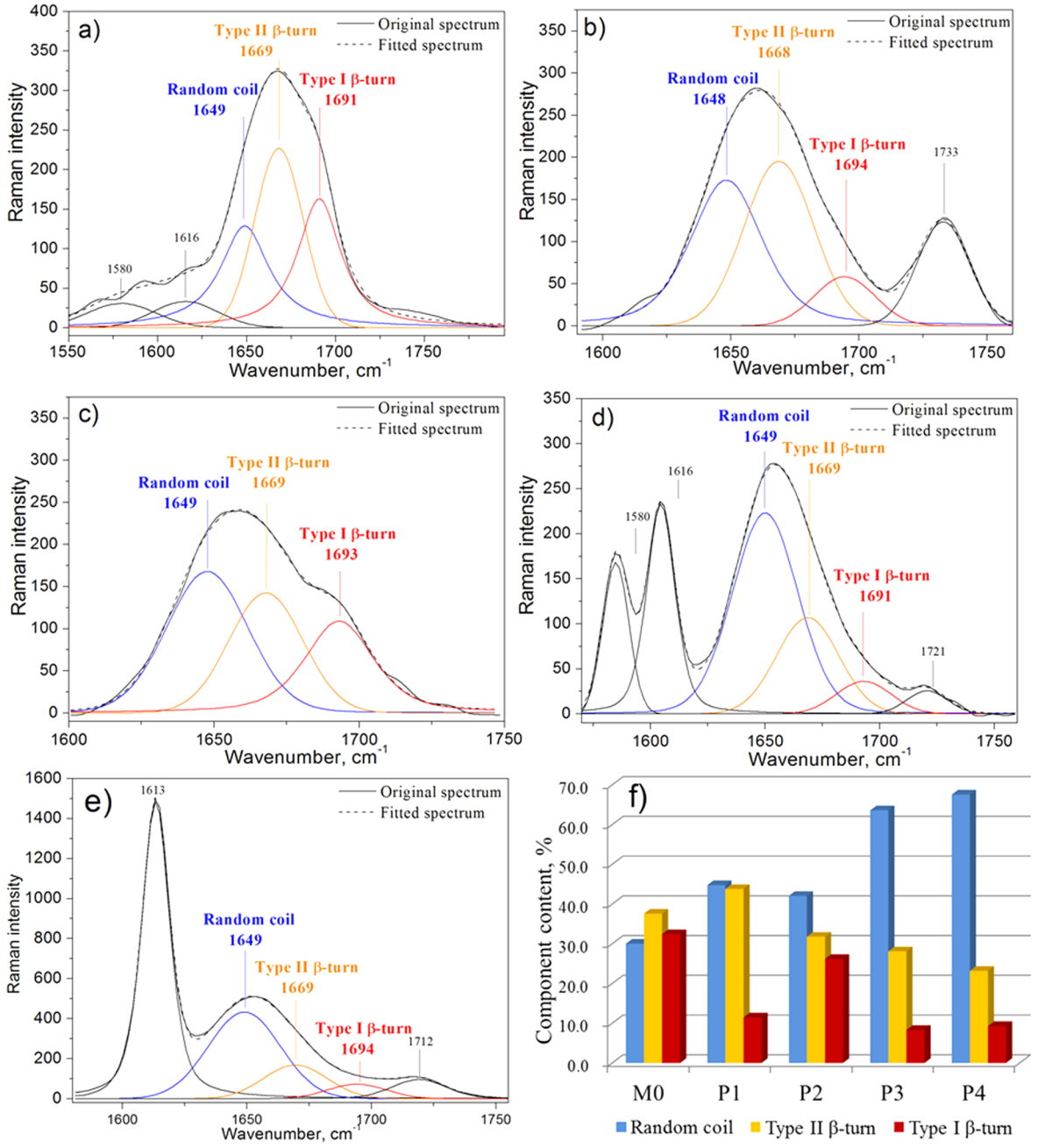


**Figure 2.** Raman spectra of pentapeptide monomer (a) **M0** and (b−e) peptidocopolymers **P1**-**P4** in bulk and (f) the spectral decomposition result.



DOI: 10.1021/acs.biomac.5b01348
*Biomacromolecules* XXXX, XXX, XXX−XXX

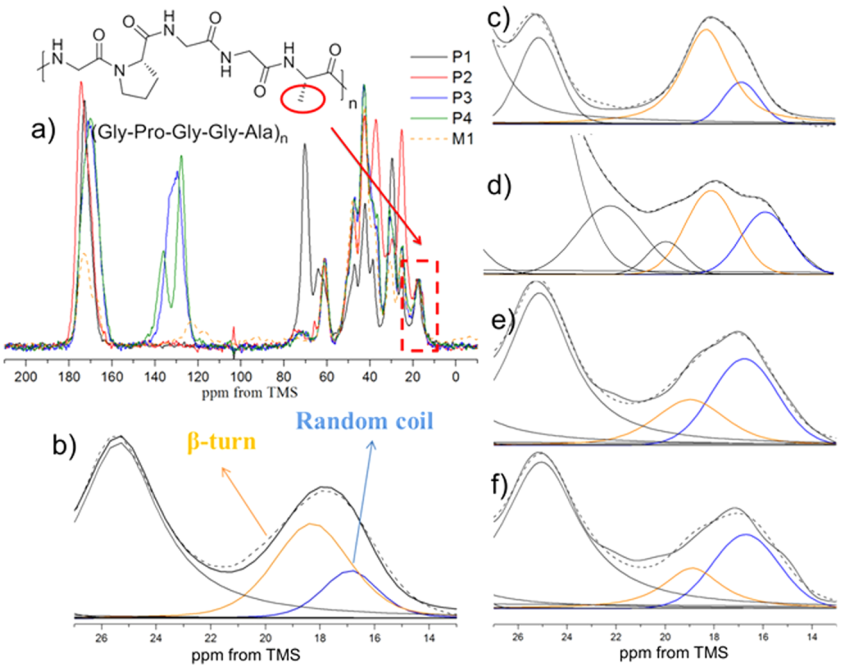


**Figure 3.** (a) Solid-state $^{13}C$ CP/MAS NMR spectra and peak fitting results of (b) **M0** and (c–f) peptidocopolymers **P1**–**P4** in bulk. The peaks in the red square in (a) have been enlarged in (b–f). The samples were lyophilized or dried under vacuum, the sample spinning rate was 10 kHz.

Information. Compared to natural silk with complicated composition,[38,39] $3_1$-helix and $\beta$-sheet conformations are less likely to occur in the proline abundant GPGGA pentapeptide. As a result, $\beta$-turn conformation can be located directly from amide I band affected by less overlapping with other components. Specifically, the location of type I, II $\beta$-turns was found around 1691 and 1669 $cm^{-1}$, respectively.[40,41] The component found around 1649 $cm^{-1}$ was likely to arise from disordered conformation or random coil according to previous studies.[23] Similarly, the three peaks were preserved after polymerization (from **P1** to **P4**) with only slight shifts (Figure 2). Assignments of these peaks are listed in Supporting Information Table S1.

On the basis of the spectral peak-fitting results, the areas of each component were normalized according to their total amide I band in order to evaluate the amount of secondary conformations of the four peptidocopolymers. Specifically, constant $\beta$-turn components of both type I and II (30% and 25%, respectively) were found in the short and flexible adipic acid-linked **P2** compared to those of **M0**, indicating the conformation of **P2** in bulk state remained similar to the elastin pentapeptide monomer. In TEG-linked copolymer **P1**, dramatic decrease of type I $\beta$-turn component compared to **M0** was observed from about 30% to less than 10%. However, the type II $\beta$-turn conformation in **P1** increased to more than 40%, even higher than that in **P2**, resulting similar total $\beta$-turn conformation ratio in both **P1** and **P2**. In short, the short and flexible adipic acid linkage in **P2** showed little influence on the secondary structure of peptidocopolymer in bulk, while the long and flexible TEG linkage limited the formation of type I $\beta$-turn, although the total $\beta$-turn conformation remained constant.

In contrast, in **P3** and **P4** when even shorter but stiff isophthalic and terephthalic linkers were introduced, the type I $\beta$-turn peak almost disappeared, while the type II $\beta$-turn peak decreased dramatically. Meanwhile, the random coil conformation increased to more than 60% in **P3** and even 70% in **P4**. The dramatically reduced content of both type I and type II $\beta$-turn in **P3** and **P4** indicated that the short and stiff hybrid linker influenced the secondary structure of peptidocopolymer more significantly than the previous flexible ones, while the structure of hybrid blocks (isophthalic for 180° linkage and terephthalic for 120°) showed no obvious influence. We supposed that the secondary structure change in **P3** and **P4** might due to the increasing rigidity of main chain, which might restrict the mobility of GPGGA block and therefore disrupt the formation of $\beta$-turn.

**Solid-state $^{13}C$ NMR of Peptidocopolymer in Bulk.** Figure 3 showed the solid-state cross-polarization magic angle spinning carbon-13 nuclear magnetic resonance (CP/MAS $^{13}C$ NMR) of the peptidocopolymers. The chemical shifts of the peptidocopolymers were mostly in agreement with those of reported $(GPGGA)_6$ polypeptide synthesized by solid-phase chemistry.[42] The Ala C$\beta$ signal (red circled in Figure 3a) is sensitive to conformational change and its chemical shift has been widely used in peptide conformation determination.[43−46] In this study, the Ala C$\beta$ chemical shift of the four peptidocopolymers was assigned at 18.25, 17.87, 16.68, and 17.03 ppm in Figure 3, which indicated different conformation between the four polymers.

To further determine the conformation difference between the four peptidocopolymers, spectral decomposition of their $^{13}C$ CP/MAS signal was performed with the results shown in Figure 3b–f. The deconvolution of Ala C$\beta$ yielded two major components around 16.8 and 18.6 ppm with different intensities. Similar to the pervious reported results of $\beta$-turn in silk, the $^{13}C$ Ala C$\beta$ chemical shift would switch to lower field due to the formation of intramolecular hydrogen bond in $\beta$-turn, which was assigned to the peak around 18.6 ppm.[27] Then the broad peak around 16.8 ppm was assigned to random coil conformation. When the integration area of each component was normalized according to the total Ala C$\beta$ signal (12–22 ppm), it was found that the component assigned


DOI: 10.1021/acs.biomac.5b01348
Biomacromolecules XXXX, XXX, XXX−XXX

as $\beta$-turn significantly decreased in **P3** (40%) and **P4** (32%) compared to those in **P1** (65%) and **P2** (55%). Although the percentage of $\beta$-turn conformation obtained in solid state NMR was different from that in Raman spectra, similar tendency was observed. In bulk, the procedure of solvent casting allowed the peptide units to arrange their conformation and possible intramolecular hydrogen bond might form. However, the linker with high rigidity and strong $\pi-\pi$ interaction in **P3** and **P4** limited the rearrangement of the pentapeptide unit, which may be one of the reasons of the decreased $\beta$-turn component.

**The Peptidocopolymers Conformation Analysis in Polar Solvents.** Water is a solvent with high polarity that largely affects secondary structure of peptide due to strong solvation effect.[47,48] Here Raman spectroscopy was again employed to study the peptide secondary structure in water with the obtained results overlaid and normalized with their corresponding results in bulk (Supporting Information Figure S14). The amide I band of the four peptidocopolymers were observed around 1650−1670 $cm^{-1}$ in water, similar to those in bulk. Specifically, the peaks of amide I band of **P2**, **P3**, and **P4** shifted to lower wavenumber, compared to their own corresponding peaks in bulk. The shift indicated that when dissolved (or fully saturated) in water, the $\beta$-turn structure was affected by solvation effect and resulted in increase of random coil conformation, which will be further supported by MD simulation result. However, no obvious peak shift was found in the amide I band of TEG-linked **P1**. The polar and hydrophilic TEG linker might act as "solvent", while the elastin pentapeptide was more likely to be "dissolved" in TEG, which made the conformation of pentapeptide in bulk and in water similar.

To gain further information on local conformation in high polarity solvent, circular dichroism (CD) spectra data were collected for the four peptidocopolymers in trifluoroethanol (TFE) due to the poor solubility of **P3** and **P4** in water. The structural feature of **M0** were reflected in the measured CD spectra by a distinct absorption at 197 nm ($\pi-\pi^*$ transition) and a medium absorption at 218 nm ($n-\pi^*$ transition) at room temperature, which were the characteristic peaks of random coil and $\beta$-turn structures, respectively.[49,50] Peptidocopolymer **P1** and **P2** showed similar CD spectrum to **M0** but with a less obvious peak at around 220 nm, indicating less $\beta$-turn conformation in polar solvents. However, strong UV absorption of aromatic ring on the main chain largely affected the CD signal from 180 to 230 nm, which resulted in very low signal-to-noise ratio (Figure 4) and little information can be obtained from the spectra of **P3** and **P4**.

**Molecular Dynamics Simulation.** Conformation of **M0** in explicit solvent was first characterized by Ramachandran plots with dihedral angles Φ2 and Ψ2, Φ3 and Ψ3 (definition shown in Supporting Information Figure S1) as reaction coordinates, as shown in Figure 5. The definition of $\beta$-turn used for MD simulation was shown in Supporting Information.[24,25] Because populations of the different states of **M0** inferred from MD sampling were in good agreement in explicit and implicit solvents (Supporting Information Table S2), implicit solvent was employed for the simulation of peptidocopolymers to allow sufficient sampling. Simulation results of **M0** showed type I and type II $\beta$-turn components around 14% and 28% respectively (Supporting Information Table S2), which was then consistent to the previous experimental results, showing the validity of simulation method used in this paper. As shown in Figure 5a, due to the steric restriction of the Pro five-membered ring Φ2

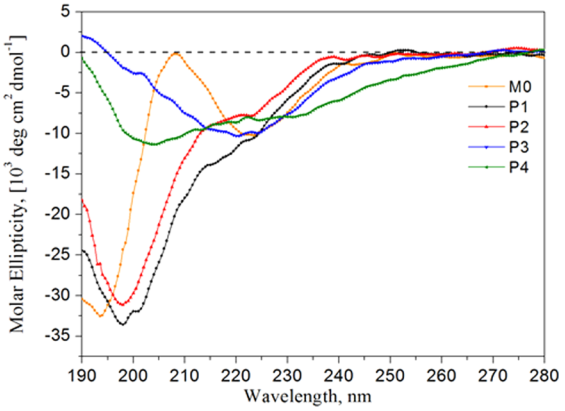


**Figure 4.** CD spectra of **M1**, **P1**−**P4** in trifluoroethanol (TFE).

mainly distributed around −120−0°, and Ψ2 distributed around −50∼10° for type I $\beta$-turn (Figure 5c) and 120∼180° for type II $\beta$-turn (Figure 5d). Similarly, Φ3 distributed around −50∼10°, Ψ3 distributed around −60∼10° for type I $\beta$-turn structure (Figure 5c), and −20∼60° for type II $\beta$-turn structure (Figure 5d) are also shown in Figure 5b. Typical conformation in Figures 5c and 4d as well as the random coil one in Figure 5e came from the MD simulation.

As a control, polypeptides $(GPGGA)_n$ ($n$ = 1, 2, 4) (for clarity, abbreviated as **P0**) without any synthetic linker were simulated, showing that the sum of type I/II $\beta$-turn possessed around 50% population among all kinds of secondary structures in which the population of type II $\beta$-turn was obviously larger than that of type I, and the total $\beta$-turn population slightly increased with the increase of repeating unit. (Figure 6a,b). Different phenomenon was found when **M2** and **M4** were integrated. From the simulation results, **P2** showed similar type I $\beta$-turn component compared to **P0**, which slightly decreased from 17 to 13% during the increase of repeating unit. Similar to **P0**, the type II $\beta$-turn component in **P2** also increased from 12 to 20% with the increase of repeating unit from 1 to 4. In contrast, both type I/II $\beta$-turn component in **P4** decreased dramatically compared to **P0** and **P2**. More specifically for **P4**, with the increase of repeating unit type I $\beta$-turn component decreased from 17 to 9%, and type II $\beta$-turn decreased from 18 to 12%. The above MD simulation results showed good agreement with the Raman and solid state NMR results in this paper. It is also worth to mention that the result indicates that the population of secondary structure for more repeating units (2 and 4 in the MD simulation) could better describe the corresponding conformation rather than one simple monomer, especially when nonpeptido elements were introduced. From the captured relatively stable conformation in MD simulation (Figure 7), **P2** showed $\beta$-turn conformation in the two repeating units, indicating less effect from the flexible linker **M2** (Figure 7a); while **P4** only retained one $\beta$-turn conformation, affected by the hydrophobic and rigid **M4** linker, which might block the intramolecular hydrogen bond and thus destabilize $\beta$-turn conformation (Figure 7b).

**Mechanical Properties.** Because the four peptidocopolymers shared similar chemical composition but tunable secondary structure, a useful insight would be provided by the investigation of their bulk mechanical properties. Films with thickness around 0.5 mm for **P1**, **P2**, **P3**, and **P4** were cast by compression molding around 90−120 °C depending on


DOI: 10.1021/acs.biomac.5b01348
Biomacromolecules XXXX, XXX, XXX−XXX

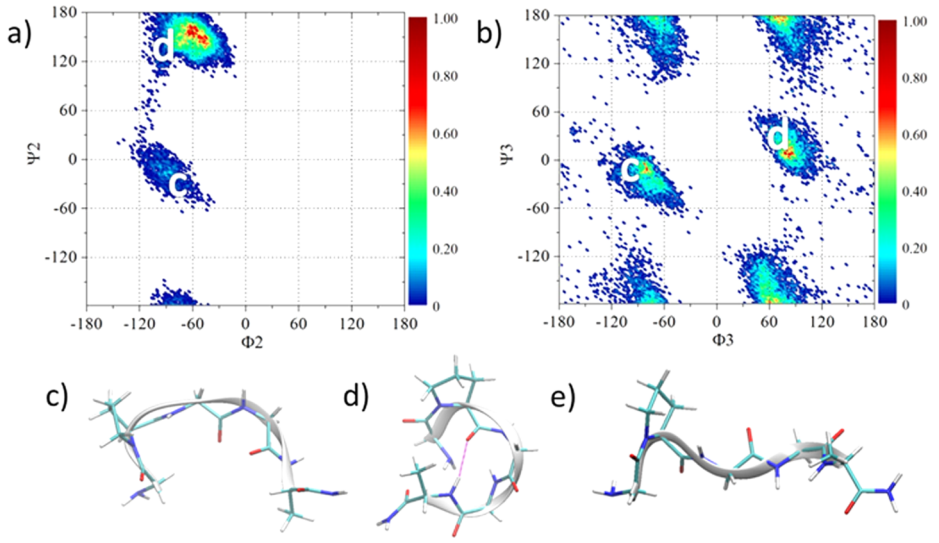


**Figure 5.** Ramanchandran plots for (a) Φ2-Ψ2 and (b) Φ3-Ψ3 pairs in **M0**. Simulated possible conformation of **M0** (c) type I $\beta$-turn, (d) type II $\beta$-turn, and (e) random coil. Labels of the $\beta$-turn conformational states, denoted as c and d correspondingly, have been placed in their respective minima.

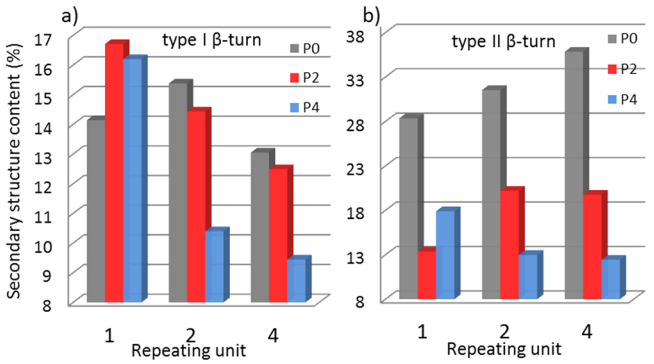


**Figure 6.** Conformation content of (a) type I $\beta$-turn, (b) type II $\beta$-turn occupancy in **P0** (black), **P2** (red) and **P4** (blue) in MD simulation. (Standard deviations less than 1%.)

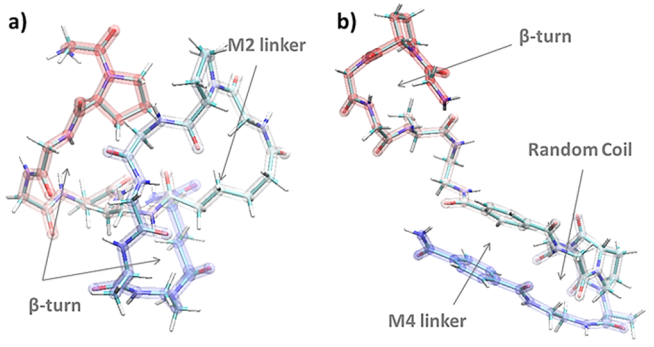


**Figure 7.** Snapshots of relativity representative conformation of (a) **P2** and (b) **P4** ($n$ = 2).

different polymers, and their tensile mechanical properties were tested in both dry and hydrated forms. Figure 8 showed the stress−strain curves of the peptidocopolymers. The dry form meant that the film was immediately subjected to mechanical testing after compress molding and vacuum drying. The four films were brittle with relatively high moduli but little extensibility. Specifically, the Young's moduli for the dry samples were 1.26, 0.58, 0.65, and 0.75 GPa for **P1**, **P2**, **P3**, and

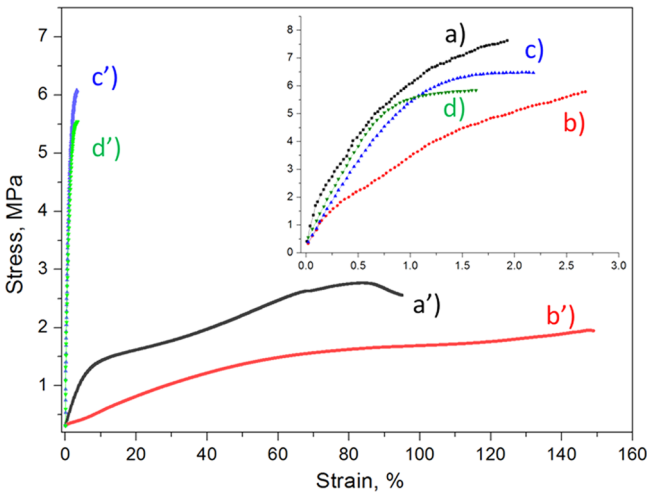


**Figure 8.** True stress−strain curves for the four peptidocopolymers in dry (inserted) and hydrated forms (a) dry **P1**; (b) dry **P2**; (a′) hydrated **P1** and (b′) hydrated **P2** with 5% water; (c) dry **P3**; (d) dry **P4**; (c′) **P3** and (d′) **P4** that were prepared with hydrated **P1** and **P2** under the same condition.

**P4**, respectively, with the maximal strains were all less than 3%. The hydrated samples were prepared by equilibrating the compressed films in air with humidity around 50−60% for about 24 h and the water content was about 5% (depending on air humidity and the time control of hydration). For **P1** and **P2**, which were easily hydrated in air, about 5% (w/w, weight of absorbed water to weight of the dry film) hydrated films were much more extensible than the dry state. While hydrated, the Young's moduli of **P1** and **P2** decreased dramatically to ∼40 and ∼10 MPa, respectively, while their extensibility were significantly increased to ∼100 and ∼150%, respectively. The synthetic **P1** and **P2** show similar properties as nature silk protein such as easily hydrated and highly elastic. However, due to the limitation of molar mass and lack of physical and chemical cross-linking, the pulled films can hardly be recovered, and the mechanical properties are much weaker then natural proteins (such as silk). In contrast, **P3** and **P4** were hardly


DOI: 10.1021/acs.biomac.5b01348
Biomacromolecules XXXX, XXX, XXX−XXX

hydrated under the same condition but exposure in air for more than 48 h led to less than 0.2% (w/w) hydration of **P3** and **P4**. The Young's Moduli of "hydrated" **P3** and **P4** films were 0.48 and 0.46 GPa, similar to those in dry state, and low maximal trains around 3−4% were found.

Interestingly, we found that the hydrated **P1** and **P2** bulk material were self-healable without pressure at room temperature (Figure 9). The 5% (w/w) hydrated **P1** and **P2** samples

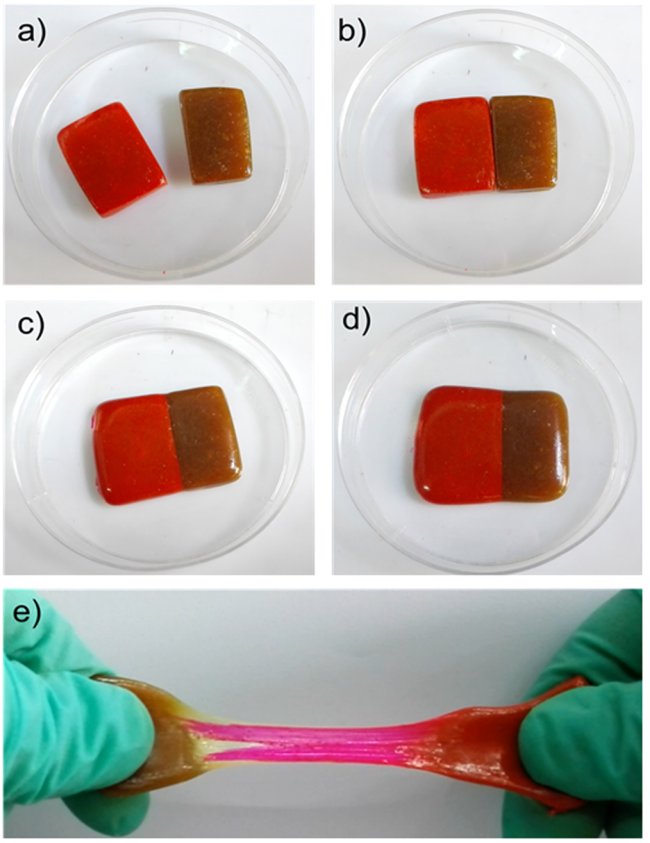


**Figure 9.** Self-healing behavior of 5% hydrated from **P2** at ambient temperature. (a) Five percent hydrated cube of **P2** (colored by Rhodamine); (b) gently brought the two pieces back to contact; (c) 24 h and (d) 48 h without any outside intervention; (e) self-healed peptidocopolymers stretched by hands.

with ca. 5 mm thickness were first cut into two pieces at room temperature. After gently bringing the two pieces back to contact, the two surfaces spontaneously self-healed under ambient condition without any other treatment. However, due to the difficulty of hydration, **P3** and **P4** showed no self-healing behavior at ambient condition and even after treatment under 100 °C with pressure between two surfaces.

According to the results from structural characterization and molecular simulation, we can easily find that **P1** and **P2** had higher content of $\beta$-turn structure. Previously it was found that $\beta$-turn was important to the hydration of proteins and renders proteins higher elasticity and ductibility, which is consistent to the mechanical performance. Moreover, the dynamic nature of hydrogen bond in **P1** and **P2** could explain the self-healing property. On the contrary, the rigid linker restricted the movement of polymer chains in **P3** and **P4**, only very few $\beta$-turn structures were retained. Thus, the self-healing property could not be observed.

## CONCLUSION

In summary, four novel bioinspired peptidocopolymers based on elastin motif pentapeptide with different small molecular linkers have been synthesized by metal-free step growth polymerization. The results indicated that the conformation, physical, and mechanical properties of the four synthesized copolymers can be tuned by different linkers. It was found that the flexible linker resulted in similar conformation and mechanical properties compared to the native protein; while the hydrophobicity and rigidity of the linker caused conformation change. The effect of different linkers to peptide conformation was further explained by MD simulation. This step-growth synthesis technique can be further applied to a broad range of monomers to achieve a simple approach toward complicated peptidocopolymer synthesis.

## ASSOCIATED CONTENT

### Supporting Information

The Supporting Information is available free of charge on the ACS Publications website at DOI: 10.1021/acs.biomac.5b01348.

Synthesis and characterization of monomers **M0**, **M1**, and **M2** and peptidocopolymers **P1**, **P2**, **P3**, and **P4**, including $^{1}$H NMR, $^{13}$C NMR as well as details of GPC-MALS, Raman, CD, DSC, and MD simulation are all available. (PDF)

## AUTHOR INFORMATION

### Corresponding Author

*E-mail: guosong@fudan.edu.cn.

### Notes

The authors declare no competing financial interest.

## ACKNOWLEDGMENTS

National Natural Science Foundation of China (Nos. 21474020, 91227203 and 51322306) and the Innovation Program of the Shanghai Municipal Education Commission are acknowledged for their financial support.

## REFERENCES

(1) Kushner, A. M.; Guan, Z. *Angew. Chem., Int. Ed.* **2011**, *50*, 9026−9057.
(2) Shu, J. Y.; Panganiban, B.; Xu, T. *Annu. Rev. Phys. Chem.* **2013**, *64*, 631−57.
(3) Lau, H. K.; Kiick, K. L. *Biomacromolecules* **2015**, *16*, 28−42.
(4) Grieshaber, S. E.; Farran, A. J.; Bai, S.; Kiick, K. L.; Jia, X. *Biomacromolecules* **2012**, *13*, 1774−1786.
(5) Biju, V. *Chem. Soc. Rev.* **2014**, *43*, 744−764.
(6) Lorenzer, C.; Dirin, M.; Winkler, A.-M.; Baumann, V.; Winkler, J. *J. Controlled Release* **2015**, *203*, 1−15.
(7) Zeng, H.; Little, H. C.; Tiambeng, T. N.; Williams, G. A.; Guan, Z. *J. Am. Chem. Soc.* **2013**, *135*, 4962−4965.
(8) Hedir, G. G.; Bell, C. A.; O'Reilly, R. K.; Dove, A. P. *Biomacromolecules* **2015**, *16*, 2049−2058.
(9) Hedir, G. G.; Bell, C. A.; Ieong, N. S.; Chapman, E.; Collins, I. R.; O'Reilly, R. K.; Dove, A. P. *Macromolecules* **2014**, *47*, 2847−2852.
(10) Nardecchia, S.; Gutierrez, M. C.; Ferrer, M. L.; Alonso, M.; Lopez, I. M.; Rodriguez-Cabello, J. C.; del Monte, F. *Biomacromolecules* **2012**, *13*, 2029−2036.
(11) Ponader, D.; Maffre, P.; Aretz, J.; Pussak, D.; Ninnemann, N. M.; Schmidt, S.; Seeberger, P. H.; Rademacher, C.; Nienhaus, G. U.; Hartmann, L. *J. Am. Chem. Soc.* **2014**, *136*, 2008−2016.



DOI: 10.1021/acs.biomac.5b01348
*Biomacromolecules* XXXX, XXX, XXX−XXX

(12) Zhang, S.; Li, Z. *J. Polym. Sci., Part B: Polym. Phys.* **2013**, *51*, 546−555.
(13) Chen, Y.; Guan, Z. *J. Am. Chem. Soc.* **2010**, *132*, 4577−4579.
(14) Yu, T.-B.; Bai, J. Z.; Guan, Z. *Angew. Chem., Int. Ed.* **2009**, *48*, 1097−1101.
(15) Rathore, O.; Sogah, D. Y. *J. Am. Chem. Soc.* **2001**, *123*, 5231−5239.
(16) Grieshaber, S. E.; Paik, B. A.; Bai, S.; Kiick, K. L.; Jia, X. *Soft Matter* **2013**, *9*, 1589−1599.
(17) Krannig, K. S.; Schlaad, H. *J. Am. Chem. Soc.* **2012**, *134*, 18542−18545.
(18) Krannig, K. S.; Sun, J.; Schlaad, H. *Biomacromolecules* **2014**, *15*, 978−984.
(19) Vacogne, C. D.; Brosnan, S. M.; Masic, A.; Schlaad, H. *Polym. Chem.* **2015**, *6*, 5040−5052.
(20) Elam, W. A.; Schrank, T. P.; Campagnolo, A. J.; Hilser, V. J. *Protein Sci.* **2013**, *22*, 405−417.
(21) Rose, G. D.; Gierasch, L. M.; Smith, J. A. *Adv. Protein Chem.* **1985**, *37*, l−109.
(22) Ding, L.; Wang, S.; Wu, W.; Hu, Y.; Yang, C.; Tan, M.; Kong, D.; Yang, Z. *Chin. J. Chem.* **2011**, *29*, 2182−2186.
(23) Hayashi, C. Y.; Lewis, R. V. *J. Mol. Biol.* **1998**, *275*, 773−784.
(24) Wasserman, Z. R.; Salemme, F. R. *Biopolymers* **1990**, *29*, 1613−1631.
(25) Zhou, C.; Leng, B.; Yao, J.; Qian, J.; Chen, X.; Zhou, P.; Knight, D. P.; Shao, Z. *Biomacromolecules* **2006**, *7*, 2415−2419.
(26) Liu, Y.; Shao, Z.; Vollrath, F. *Biomacromolecules* **2008**, *9*, 1782−1786.
(27) Liu, Y.; Sponner, A.; Porter, D.; Vollrath, F. *Biomacromolecules* **2008**, *9*, 116−121.
(28) Roth, P. J.; Wiss, K. T.; Zentel, R.; Theato, P. *Macromolecules* **2008**, *41*, 8513−8519.
(29) Nilles, K.; Theato, P. *Eur. Polym. J.* **2007**, *43*, 2901−2912.
(30) Günay, K. A.; Theato, P.; Klok, H.-A. *J. Polym. Sci., Part A: Polym. Chem.* **2013**, *51*, 1−28.
(31) Duan, Y.; Wu, C.; Chowdhury, S.; Lee, M. C.; Xiong, G.; Zhang, W.; Yang, R.; Cieplak, P.; Luo, R.; Lee, T.; Caldwell, J.; Wang, J.; Kollman, P. *J. Comput. Chem.* **2003**, *24*, 1999−2012.
(32) Guvench, O.; Hatcher, E.; Venable, R. M.; Pastor, R. W.; MacKerell, A. D., Jr. *J. Chem. Theory Comput.* **2009**, *5*, 2353−2370.
(33) Van Der Spoel, D.; Lindahl, E.; Hess, B.; Groenhof, G.; Mark, A. E.; Berendsen, H. J. C. *J. Comput. Chem.* **2005**, *26*, 1701−1718.
(34) Hess, B.; Kutzner, C.; Van Der Spoel, D.; Lindahl, E. *J. Chem. Theory Comput.* **2008**, *4*, 435−447.
(35) Case, D. A.; Darden, T. A.; Cheatham, T. E.; Simmerling III, C. L.; Wang, J.; Duke, R. E.; Luo, R.; Walker, R. C.; Zhang, W.; Merz, K. M., et al. *AMBER11* ; University of California: San Francisco, 2010.
(36) Jorgensen, W. L.; Chandrasekhar, J.; Madura, J. D.; Impey, R. W.; Klein, M. L. J. *J. Chem. Phys.* **1983**, *79*, 926−935.
(37) Rousseau, M.-E.; Lefèvre, T.; Beaulieu, L.; Asakura, T.; Pézolet, M. *Biomacromolecules* **2004**, *5*, 2247−2257.
(38) Lefèvre, T.; Rousseau, M.-E.; Pézolet, M. *Biophys. J.* **2007**, *92*, 2885−2895.
(39) Lefèvre, T.; Paquet-Mercier, F.; Rioux-Dubé, J.-F.; Pézolet, M. *Biopolymers* **2012**, *97*, 322−336.
(40) Hutchinson, E. G.; Thornton, J. M. *Protein Sci.* **1994**, *3*, 2207−2216.
(41) Krimm, S.; Bandekar, J. *Biopolymers* **1980**, *19*, 1−29.
(42) Ohgo, K.; Kawase, T.; Ashida, J.; Asakura, T. *Biomacromolecules* **2006**, *7*, 1210−1214.
(43) Asakura, T.; Okushita, K.; Williamson, M. P. *Macromolecules* **2015**, *48*, 2345−2357.
(44) Asakura, T.; Yao, J.; Yamane, T.; Umemura, K.; Ulrich, A. S. *J. Am. Chem. Soc.* **2002**, *124*, 8794−8795.
(45) Ruan, Q.; Zhou, P.; Hu, B.; Ji, D. *FEBS J.* **2008**, *275*, 219−232.
(46) Yao, T.; Jiang, T.; Pan, D.; Xu, Z.-X.; Zhou, P. *RSC Adv.* **2014**, *4*, 40273−40280.
(47) Huang, W.; Krishnaji, S.; Tokareva, O. R.; Kaplan, D.; Cebe, P. *Macromolecules* **2014**, *47*, 8107−8114.
(48) Huang, W.; Krishnaji, S.; Tokareva, O. R.; Kaplan, D.; Cebe, P. *Macromolecules* **2014**, *47*, 8098−8106.
(49) Nuhn, H.; Klok, H.-A. *Biomacromolecules* **2008**, *9*, 2755−2763.
(50) Kojima, C.; Irie, K.; Tada, T.; Tanaka, N. *Biopolymers* **2014**, *101*, 603−612.


DOI: 10.1021/acs.biomac.5b01348
*Biomacromolecules* XXXX, XXX, XXX−XXX